



Synoptic TeV Gamma Ray Observatories: Recent Results and Future Plans

GUS SINNIS¹

¹*Physics Division, Los Alamos National Laboratory, Los Alamos, NM USA*

Gus@lanl.gov

Abstract. Extensive air shower arrays directly detect the particles in an extensive air shower that reach the observation altitude. This detection technique effectively makes air shower arrays synoptic telescopes - they are capable of simultaneously and continuously viewing the entire overhead sky. Typical air shower detectors have an effective field-of-view of 2 sr and operate 95% of the time. These two characteristics makes them ideal instruments for studying the highest energy gamma rays, extended sources, and transient phenomena. Until recently air shower arrays have been plagued by poor sensitivity - resulting in few detections from these types of instruments. Over the past five years, the situation has changed markedly. Milagro, in the U.S, and the Tibet AS γ array in Tibet, have detected very-high-energy gamma-ray emission from the Crab Nebula and the active galaxy Markarian 421 (both previously known sources). Milagro has discovered TeV diffuse emission from the Milky Way, three unidentified sources of TeV gamma rays, and several candidate sources of TeV gamma rays. Building upon the success of Milagro and Tibet AS γ , the future development path is clear. A water Cherenkov detector placed at an extreme altitude would have unique capabilities and holds the promise of revealing the transient TeV universe. Here I will review the achievements of the current generation of air shower detectors and discuss the near and long-term future of this class of instruments.

Introduction

The first generation of extensive air shower arrays to be used for gamma-ray astronomy were typically composed of small plastic scintillators ($\sim 1 \text{ m}^2$ each) distributed over large areas (40,000 - 230,000 m^2). With an active area comprising $< 1\%$ of the enclosed area these arrays had high energy thresholds ($\sim 100 \text{ TeV}$), which limited their sensitivity. The CYGNUS [1] and CASA [2] arrays were the largest of these type of instruments. The energy threshold of the CASA array was $\sim 200 \text{ TeV}$, making extragalactic astronomy impossible and Galactic astronomy difficult. No unequivocal evidence for sources of gamma rays was found with these instruments. The path forward from this generation of instruments was clear - lower the energy threshold. Two different approaches have been successfully employed to accomplish this goal. The Milagro detector [3] in Los Alamos, NM uses the water Cherenkov technique to provide an active detector area that is essentially equal to the physical area enclosed by the detector. This

dense sampling of the air shower yields a median energy of $\sim 2 \text{ TeV}$ to gamma rays from a Crab-like source. The Tibet AS γ detector [4] in Tibet has obtained a similar energy response by locating their telescope at an extreme altitude - 4300 m above sea level. The low-energy threshold of these instruments has enabled high significance detections of the Crab Nebula and the extragalactic source Mrk 421, an active galaxy at a redshift of 0.03.

Extensive air shower (EAS) arrays have the advantage of time on source over imaging air Cherenkov telescopes (IACTs). Whereas a deep observation for an IACT may be 50-100 hours over a period of one to several years, an EAS array views every object in $\sim 2\pi \text{ sr}$ of the sky for ~ 1400 hours per year. While this does not make up for the comparatively poor angular resolution of the EAS arrays for studying point sources, for sources that are large compared to the angular resolution of IACTs this becomes a significant advantage.

In addition to detecting and studying known sources of VHE gamma rays, the promise of EAS arrays lies in their ability to discover new sources

and to study the long-term evolution of VHE gamma-ray sources. The current instruments have partially fulfilled this promise with the discovery of extended sources. However they appear to lack the sensitivity required to carry out a vigorous program of discovery and study of extragalactic sources. There are plans for future instruments that can attain the requisite level of sensitivity to achieve these goals.

In this paper I will review the recent achievements of the current generation of synoptic telescopes and draw a roadmap for the future development of high sensitivity synoptic VHE telescopes.

Current synoptic TeV gamma-ray observatories

There are three major EAS in operation today: Milagro, the Tibet AS γ , and ARGO (Astrophysical Radiation with Ground-based Observatory). Milagro (Fig. 1) consists of a central water reservoir covering an area of $\sim 4000 \text{ m}^2$, surrounded by an array of 175 water tanks covering an area of $\sim 34,000 \text{ m}^2$ (the outrigger array). The central detector has dimensions $80\text{m} \times 50\text{m}$ with a depth of 8m at the center. The reservoir is instrumented with 750 20cm photomultiplier tubes (PMTs) arranged in two layers. The top layer of 450 PMTs is under 1.4m of water and the bottom layer of 273 PMTs is under 6m of water. Both layers are on a $2.8\text{m} \times 2.8\text{m}$ grid. The entire reservoir is enclosed with a light-tight cover. Each water tank has an area of 8m^2 and a depth of $\sim 1\text{m}$. They are instrumented with a single PMT that is mounted at the top looking down into a TYVEK lined water volume. The PMTs in the top layer and the outrigger array are used to reconstruct the direction of the primary gamma ray (or cosmic ray) to an accuracy of ~ 0.5 degrees. The bottom layer is used to discriminate against the background cosmic radiation. Air showers induced by hadrons contain a penetrating component (muons and hadrons that shower in the reservoir). This component results in a compact bright region in the bottom layer of PMTs (see [3]) for details. A cut based on the distribution of light in their bottom layer removes 90% of the background cosmic rays while retaining 50% of the gamma ray events. The trigger rate (before

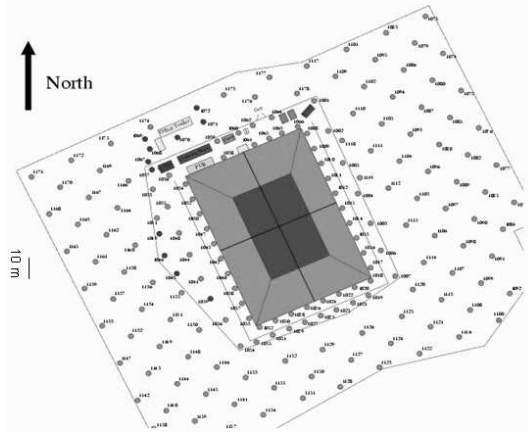


Fig. 1. The Milagro observatory. The central shaded region is a 24 million liter water reservoir. The reservoir is surrounded by an array of small water tanks. See text for details.

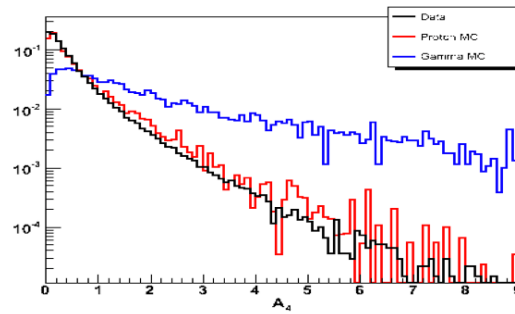


Fig. 2. The A_4 parameter used by Milagro to distinguish gamma rays from the cosmic-ray background. The solid blue line shows the distribution for gamma ray events, the red line for proton events, and the black line for data.

background rejection) is $\sim 1700 \text{ Hz}$. More recently the collaboration has developed a background rejection method that utilizes the information in the array of outrigger tanks. This improves the sensitivity of Milagro by a factor of ~ 2 . The parameter is known as A_4 , and the distribution of Monte Carlo gamma rays, protons, and data are shown in Fig. 2. The efficacy of the new cut improves markedly with energy and gives Milagro unprecedented sensitivity at the highest energies.

Tibet AS γ (Fig. 3) is a more traditional scintillator array located at an altitude of 4300m a.s.l. The detector has undergone significant upgrades over the past decade and is currently composed of 789 scintillation counters on a 7.5m grid. Each

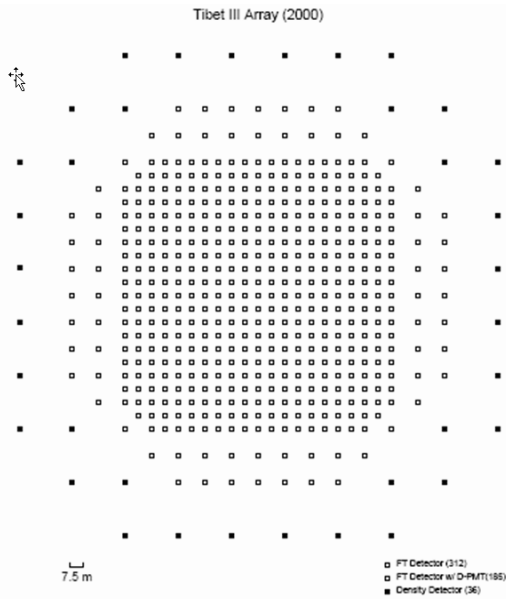


Fig. 3. A schematic drawing of the Tibet AS γ array.

counter consists of a 0.5m² plastic scintillator viewed by a 5cm PMT. Each detector is covered with a 5mm sheet of lead. The total area enclosed by the array is 36,900 m². The trigger rate is 1700 Hz and the angular resolution is 0.9 degrees.

Both Milagro and AS γ have demonstrated their sensitivity with detections of the Crab Nebula. AS γ has reported two independent detections of the Crab Nebula. In data taken between 1996 and 1999 they reported a 5.5σ detection with a less sensitive instrument, the HD array [5]. With the Tibet-III detector they report a 4.8σ detection with 1.5 years of running time [6]. This sensitivity on the Crab Nebula ($4\sigma/\sqrt{yr}$) is comparable to that of the Milagro detector before the construction of the outrigger array. Milagro now reports a sensitivity of $\sim 8\sigma/\sqrt{yr}$ with the outrigger array [7]

The ARGO detector (see Fig. 4) is also located at the Yangbajing cosmic-ray observatory in Tibet. ARGO is a dense sampling array with 92% sensitive area over a 5,772 m² area and a total area of 11,000 m². The particle detectors in ARGO are resistive plate chambers (RPCs) - a parallel plate gas chamber. In ARGO each RPC is composed of 10 pads each of which contains 8 detector strips. The spatial resolution is determined by the geometry of the strips and is 6.7 cm in one direction and 62 cm

in the perpendicular direction. The time resolution of the RPCs is about 1 ns, similar to that of scintillation counters. The RPCs are arranged in groups of 12 (a cluster) and there will be a total of 154 clusters in the complete detector. As of the summer of 2007 there were 130 clusters operational covering an area of ~ 5800 m² [8]. Since the detectors are thin there is no possibility to distinguish the passage of muons, however the ARGO collaboration expects to utilize the fine spatial resolution and dense sampling to distinguish air showers generated by gamma rays from those generated by hadronic cosmic rays. With an angular resolution of ~ 0.5 degrees and a median energy of triggered gamma rays below 1 TeV ARGO should have the sensitivity to detect the Crab Nebula at 10 standard deviations in one year of observation without background rejection and 15σ with its background rejection capabilities. At this conference the ARGO collaboration presented preliminary results on the Crab Nebula and the active galaxy Mrk 421 [8].

Sky Surveys

One of the primary motivations for a synoptic instrument is to perform an unbiased sky survey. Both Milagro [9] and Tibet [13] have surveyed the Northern sky for point sources of TeV gamma rays. Fig. 5 shows a more recent map made by the Milagro collaboration. Both the Crab Nebula and the active galaxy Mrk 421 are clearly visible in this map. Excluding these sources the distribution of significances is well fit by a Gaussian with unit width and zero mean. Therefore we know that there are no steady point sources in the Northern hemisphere with a flux greater than 200-600 mCrab (depending upon position in the sky) [9]. However, there are two interesting regions in this map. After the Crab Nebula and Mrk 421, the brightest point in the Milagro survey has a position of RA=79.9°, $\delta=26.8^\circ$. This position was previously reported by the Milagro collaboration as the second brightest point in the Northern hemisphere [10]. It is also coincident with the location of an EGRET unidentified object. However a follow-up search by the Whipple collaboration [11] failed to detect a point source at this location. The next brightest location is in the Cygnus region of the Galaxy and was also noted by the Tibet array. This

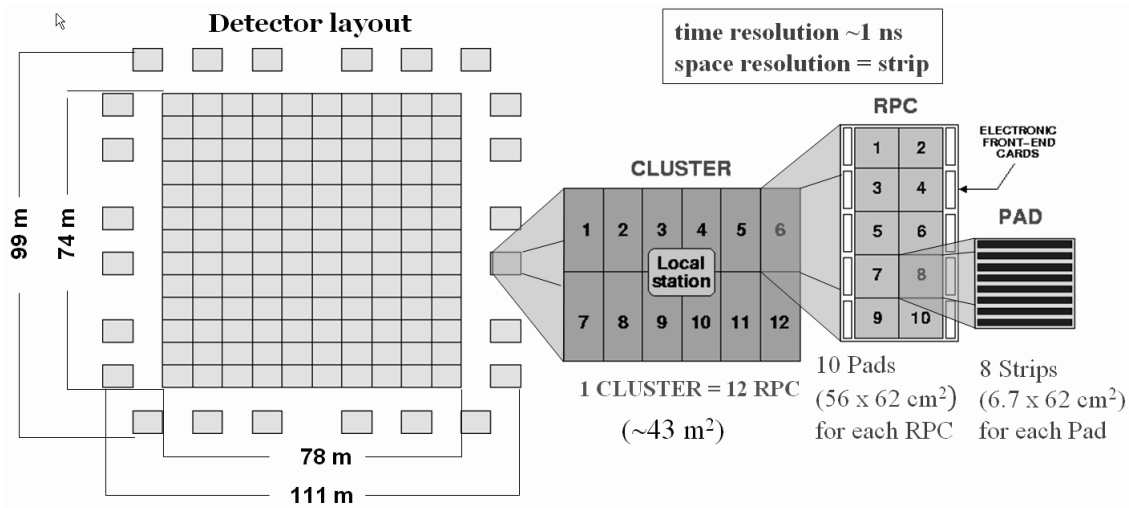


Fig. 4. A schematic drawing of the ARGO detector

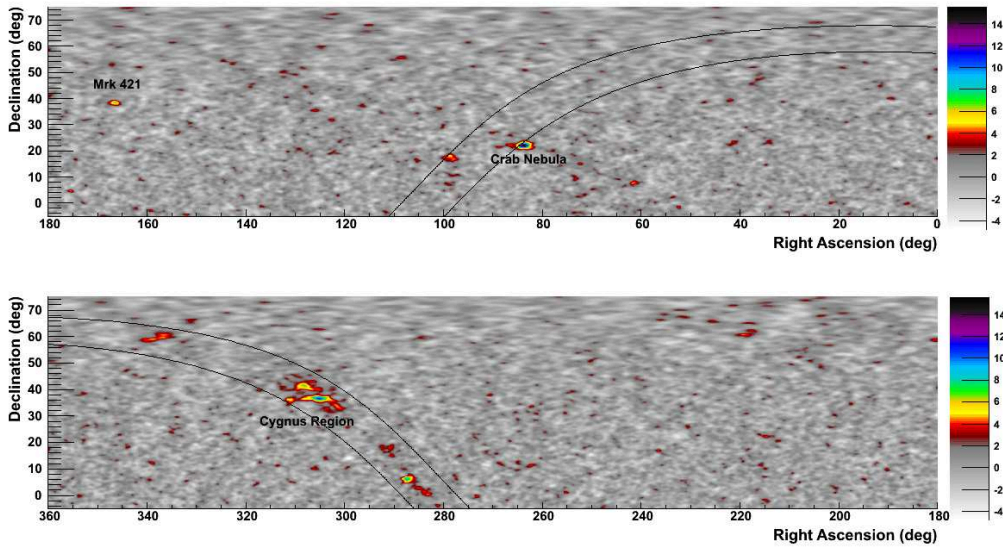


Fig. 5. Map of the Northern hemisphere in TeV gamma rays (the Milagro collaboration) with 2.1 degree smoothing (optimized for point sources). The color scale is standard deviations of the excess (integrated over a 2.1 degree bin) at the location. The coordinates are right ascension along the x-axis and declination along the y-axis. The solid black lines are drawn ± 5 degrees around the Galactic plane.

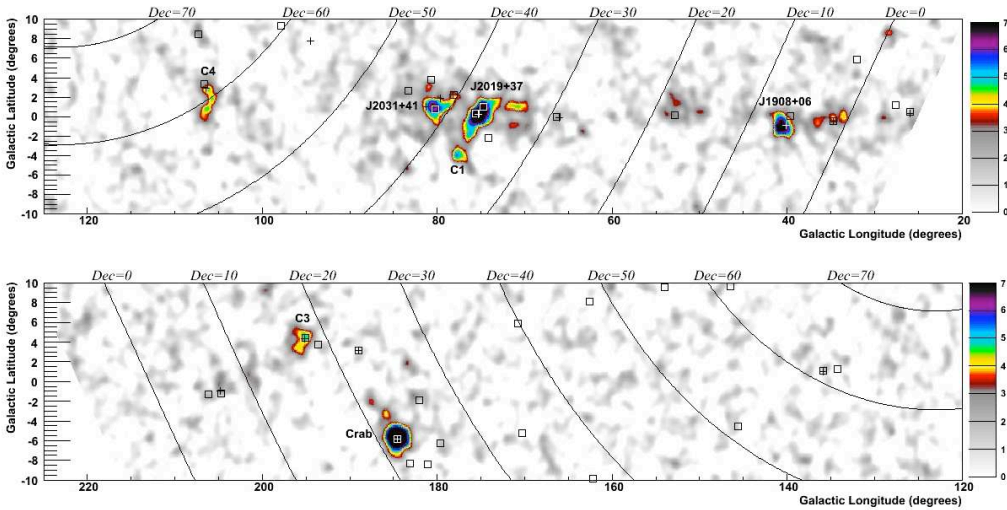


Fig. 6. The Galaxy in TeV gamma rays from Galactic longitude 20 degrees to 220 degrees and Galactic latitude from -10 degrees to 10 degrees. The image is the culmination of a seven year exposure by the Milagro instrument. The color scale shows the statistical significance of the observed excess (over the cosmic-ray background) at each point. Crosses mark the location of GeV sources and boxes mark the location of sources in the 3EG catalog. Locations marked as C1, C3, & C4 are candidate sources as determined by Milagro and the three locations marked as JXXXX+YY are sources discovered by Milagro. To improve the clarity of the figure significances above 7 standard deviations are shown as black and those below 3 standard deviations are shown as a monochrome.

coincidence was first pointed out by Walker et al. [12] along with a statistical analysis that showed a significant correlation between the $> 4\sigma$ regions in the Milagro and Tibet surveys (not including the Crab Nebula and Mrk 421). Further discussion of these regions is given below.

Galactic Plane Survey

The Milagro sky survey shows clear evidence for TeV gamma ray sources localized to the Galactic plane. Fig. 6 shows a more detailed view of the Milky Way in TeV gamma rays. The range of Galactic longitude visible is limited by the latitude of the Milagro observatory and a requirement that events fall within 45 degrees of zenith to be considered in the analysis. The boxes mark the locations of EGRET sources (from the 3rd EGRET catalog [14]) and the crosses mark the locations of GeV gamma-ray sources identified by EGRET [16]. The sensitivity of this survey is between 3 and $6 \times 10^{-15} \text{ TeV}^{-1} \text{ cm}^{-2} \text{ s}^{-1}$ [17] at 20 TeV. There are a total of 8 regions with an excess above background of over 4.5 standard deviations (including the Crab Nebula) [note: candidate source

C2 is not labeled in Fig. 6]. Table 1 gives relevant information for these 8 sources [7]. Those regions with a significance over 5 standard deviations after trials are identified as new sources and given an MGRO JXXXX+XX designation. Otherwise the region is called a source candidate and labeled Cn. We discuss details of each source below.

There are several noteworthy features of these new TeV sources all of which are consistent with the interpretation that these new TeV sources are pulsar wind nebula (PWN).

- This is a high-energy survey therefore these sources must have relatively hard spectra. The differential spectral index that connects these measurements with EGRET measurements (when there is an EGRET counterpart) is -2.3.
- Many of the sources are extended, with large extents by TeV standards.
- There is a strong correlation between these sources and the EGRET GeV catalog. Excluding the Crab Nebula there are 13 GeV sources within this survey area. Five of the seven sources and source candidates lie

within a 3x3 degree box centered on the EGRET GeV sources. The chance probability of such an occurrence is 3×10^{-6} .

Source Candidate C4

This region is coincident with the Boomerang PWN and a GeV source. This clearly an extended source and the significance increase to 6.3 standard deviations(pre-trial) in a 3x3 degree bin. The >100 MeV emission detected by EGRET has a very similar extended structure to that observed by Milagro at 20 TeV.

The Cygnus Region

The region spanning Galactic longitude 70 and 85 degrees is known as the Cygnus Region after the eponymous constellation located in the area. From the Earth this direction is along the spiral arm of the Galaxy in which we reside. Therefore we are looking into a large column density and at relatively nearby objects ($\sim 1-2$ kpc). The region contains several potential cosmic-ray acceleration sites - Wolf-Rayet stars [18], OB associations [19], and supernova remnants [20]. In addition there is an unidentified TeV source, TeV J2032+413 [15] and 4 GeV sources [16]. Milagro has identified two definite sources and 2 source candidates in this region. Fig. 7 shows a the TeV emission from the Cygnus Region (as observed by Milagro), along with the locations of hotspots identified by the Tibet AS γ array.

The brightest TeV source in this region is MGRO J2019+37 [21, 17]. As seen from Fig. 7 this source has also been detected by the Tibet AS γ observatory. The position of the TeV MGRO J2019+37 is consistent with PWN G75.2+0.1 and with the blazar B2013+370 [22]. Given the angular size of the TeV source and the high-energy emission it is unlikely that the blazar is the TeV source.

The location of MGRO J2031+41 is consistent with the previously reported position of TeV J2032+413 discovered by the HEGRA collaboration [23]. However the flux at 20 TeV is about a factor of three higher than a straightforward extrapolation of the flux of TeV J2032+413 measured by HEGRA (up to 10 TeV). Thus, it is likely that this is a new source.

Source candidate C2 is part of a complicated region. With a large matter density the contribution from a diffuse component is expected to be large and the nearby extended source J2019+37 (with a poorly measured morphology) it is not clear that there is a new point or extended source of TeV gamma rays at this location. Given the low statistical significance of the detection and the complications of the gamma-ray background in the region it is likely that this excess is due to a statistical fluctuation of the gamma-ray background. On the other hand the source candidate C1 is more interesting. Aside from C2 this is the only source not coincident with a GeV source (or any EGRET source) and it is far enough from the Galactic plane (~ 4 degrees) that the Galactic diffuse emission is small at TeV energies. The apparent confirmation of the source by the Tibet observatory (note: an exact calculation of a “post-trials” significance of the Tibet observation is difficult and will not be attempted here) seems to indicate that this is a true TeV source. Follow-up observations by the VERITAS instrument will be crucial for resolving the nature of this source.

MGRO J1908+06

This is perhaps the most exciting of the sources discovered by an all-sky TeV instrument. The H.E.S.S. collaboration has performed follow-up observations of this source and report a significant detection [24]. H.E.S.S. measures a very hard spectrum, with a differential spectral index of -2.05 between 400 GeV and 30 TeV. The flux at 20 as measured by H.E.S.S. is in excellent agreement with the flux reported by Milagro. Because of the low declination of this source (and subsequently the large zenith angle of the Milagro observations) the actual median energy of the Milagro detection is ~ 50 TeV. MRGO J1908+06 may be the highest energy gamma-ray emitter observed to date and is an excellent candidate for a cosmic-ray accelerator. A more detailed analysis of the energy spectrum - in particular at the highest possible energies, >100 TeV, is needed.

C3

This source candidate is coincident with the Geminga gamma-ray pulsar, the second brightest

Object Name	Location	Significance	Flux ($\times 10^{-15} \text{TeV}^{-1} \text{cm}^{-2} \text{s}^{-1}$)	Extent
Crab Nebula	184.5, -5.7	15.0	10.9 ± 1.2	...
MGRO J2019+37	75.0, 0.2	10.4	8.7 ± 1.4	1.1 ± 0.5
MGRO J1908+06	40.4, -1.0	8.3	8.8 ± 2.4	< 2.6
MGRO J2031+41	80.3, 1.1	6.6	9.8 ± 2.9	3.0 ± 0.9
C1	77.5, -3.9	5.8	3.1 ± 0.6	< 2.0
C2	76.1, -1.7	5.1	3.4 ± 0.8	...
C3	195.7, 4.1	5.1	6.9 ± 1.6	2.8 ± 0.8
C4	105.8, 2.0	5.0	4.0 ± 1.3	3.4 ± 1.7

Table 1. Results of the Milagro Galactic Plane Survey. Locations are given in Galactic coordinates (longitude, latitude), the significance is pre-trial, the flux is at 20 TeV and the extent is the diameter of the object measured in degrees.

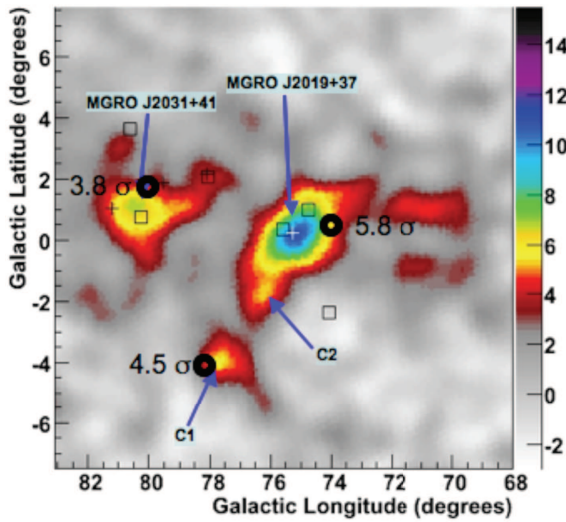


Fig. 7. The Cygnus Region as seen in TeV gamma rays. The color scale represents observations from the Milagro observatory. The black annuli are locations of hot spots in the region detected by the Tibet AS γ observatory. The marked significances are also from the Tibet AS γ .

GeV gamma-ray source in the sky. At ~ 170 pc from earth Geminga would be the closest TeV source to earth. The angular size measured by Milagro implies a source diameter of ~ 8 pc.

Diffuse TeV Gamma-Ray Emission

In addition to the sources discussed above Fig. 6 shows the presence of a diffuse gamma-ray flux from the Galaxy, especially near the Cygnus Region and at lower Galactic longitude (near MGRO J1908+06). This diffuse emission is due to the interaction of cosmic-ray nuclei with matter and inverse Compton interactions of high-energy electrons with lower energy (infrared, optical, and cos-

mic microwave background) photons. Thus, the measurement of the diffuse gamma-ray emission from our Galaxy yields information about the intensity and spectrum of cosmic rays (including high-energy electrons) far from the earth. Lower energy measurements by the EGRET showed clear evidence of an excess (over predictions based upon the matter density and the local cosmic-ray intensity and spectrum) above 1 GeV [25]. Explanations of this GeV excess range from the annihilation of dark matter particles [26] to a varying cosmic-ray spectrum and/or intensity across the Galaxy [27, 28, 29]. A model has been developed (GALPROP [27]) to predict the diffuse emission at earth based upon the matter density in the Galaxy, the interstellar radiation field, and the cosmic-ray spectra of protons, electrons, and heavy elements. To account for the GeV excess an “optimized” model was developed where the contribution from the inverse Compton component was increased to account for the GeV excess. (The original GALPROP model is referred to as the conventional model below.) While this increase is relatively small at GeV energies, it predicts that at TeV energies the inverse Compton component dominates over the pion component. (The pion component arises from the interaction of hadronic cosmic rays with matter.) Therefore, if this interpretation is correct, measurements of the diffuse gamma radiation at 10 TeV are indicative of the ~ 100 TeV electron spectrum at distant locations within the Galaxy. Fig. 8 shows the diffuse TeV gamma-ray flux and the predictions of both the conventional and optimized GALPROP models. The data shown in the figure have had the contributions from the sources discussed above removed, and thus represent the diffuse flux (in the absence of other as yet unresolved sources). Note

that even the optimized version of GALPROP under predicts the TeV flux by a factor of 2.7 in the Cygnus Region. The excess above the GALPROP prediction has a statistical significance of roughly 3 standard deviations. This excess could be explained by the existence of a cosmic-ray accelerator within the Cygnus Region. This would lead to a harder spectrum of cosmic rays within this region and therefore a larger flux of high-energy gamma rays. Alternatively, the excess could be explained by unresolved point sources of TeV gamma rays that may lie within the Cygnus Region. This resolution of this question awaits more detailed follow-up observations by the VERITAS gamma-ray telescope.

Anisotropy of the Cosmic Radiation

While several groups have previously reported measurements of cosmic-ray anisotropy (see [31] for a review), these measurements have been one-dimensional, i.e. anisotropy as a function of right ascension. Recently, this situation has changed and current experiments now have the statistical power to make 2-dimensional maps of the anisotropy of cosmic rays in the energy range from 1-100 TeV. The Tibet AS γ observatory has produced the first such map showing the anisotropy of the cosmic radiation in two dimensions [32], see Fig. 9. There are two striking features of this map: the large deficit near a right ascension of 180 degrees (Region I in the figure) and the excess between right ascension 50 and 70 degrees (Region II in the figure). The cosmic-ray intensity in the region of the deficit is 0.998 that of the average cosmic-ray intensity and in the region of the excess about 1.003 times that of the average cosmic-ray intensity. The direction of the deficit is the direction perpendicular to the Galactic plane. Despite their ability to observe these anisotropies, the Tibet group failed to detect the Compton-Getting effect. First predicted by Compton in 1935 [33] this effect is due to the earth's motion through a cosmic-ray gas at rest with respect to the Galaxy. The non-observation of the effect is evidence that the cosmic rays co-rotate with the matter in our spiral arm of the Galaxy. While the direction of the excess in Region II is consistent with the "tail-in" region of the heliosphere, the direction of open magnetic field lines

(opposite to the direction of motion of the Sun through the local interstellar medium). Also evident in Fig. 9 is a smaller excess in Region III. This region is in fact the Cygnus Region and given the observations discussed above it is likely that the observed excess is due to gamma rays from the Cygnus Region and the fractional excess observed by the Tibet AS γ is consistent with the gamma-ray flux reported by Milagro from the entire region.

The Tibet observatory does not have the ability to distinguish gamma rays from cosmic rays, therefore their observation alone does not fully constrain the possible explanations for the excesses. Milagro has made similar observations and by examining their data both with and without a cut on the hadronic background can determine if the excess is due to cosmic rays or gamma rays. Utilizing all of the Milagro data (no background rejection cut applied) yields an excess comparable to (but somewhat smaller than) that observed by the Tibet array. Fig. 10 shows the fractional excess observed by Milagro as a function of the cut on the A4 parameter. For comparison, the fractional excess is also shown for the Crab Nebula. It is clear from this figure that the excess is from Region II is due to a true anisotropy in the cosmic radiation and can not be explained by a gamma ray source [34]. While the observations themselves are of high statistical significance (over 15 standard deviations for both the Tibet observation and the Milagro observation), the interpretation of these observations is still a matter of considerable debate.

Future Directions

Given the joint success of both the Milagro and Tibet observatories it is natural to consider future improvements to all-sky TeV gamma-ray observatories. A straightforward approach to improving the sensitivity of a future instrument is to combine the two critical features of the two instruments - the high altitude of the Tibet array and the use of water Cherenkov technology to detect the air shower as it hits the ground. This is the approach taken by the High Altitude Water Cherenkov (HAWC) collaboration [35]. An alternative approach is to dramatically improve the response at the highest energies. This can be achieved by constructing a large area muon detector within a large ($\sim 100,000 \text{ m}^2$)

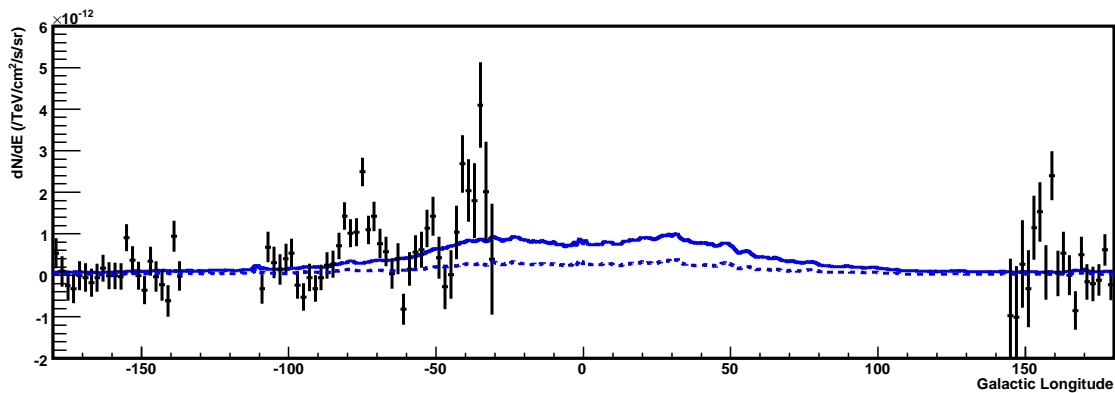


Fig. 8. The longitudinal profile of the Galactic diffuse emission of TeV gamma rays measured by the Milagro observatory [30]. The solid line shows the prediction of the “optimized” GALPROP model (increased inverse Compton component to fit EGRET data) and the dashed line shows the prediction of the “conventional” GALPROP model (cosmic-ray intensity and spectrum assumed to be the same as measured at earth). Note that even the optimized model under predicts the TeV measurement in the Cygnus Region.

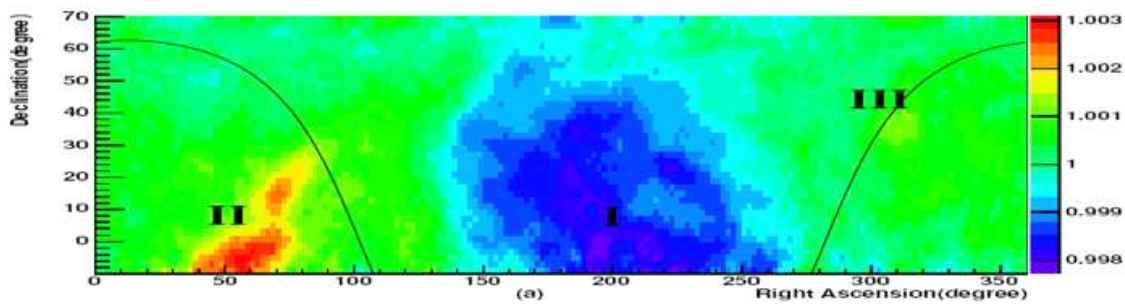


Fig. 9. The anisotropy in the cosmic radiation as measured by the Tibet AS γ observatory. This is the first two-dimensional map of high statistical significance of the cosmic-ray anisotropy. Region III is the Cygnus Region and the observed excess in that direction is consistent with the gamma-ray flux measured by Milagro in that direction.

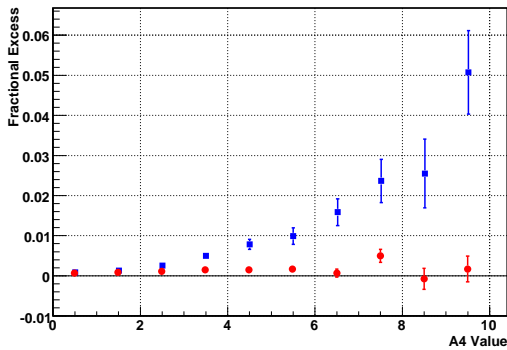


Fig. 10. The fractional excess observed by Milagro as a function of the cut on the A4 parameter for Region II (blue markers). Shown for comparison is the dependence of the excess from the Crab Nebula (red markers).

air shower array. This is the approach taken by the Tibet with Muons concept.

The HAWC collaboration is proposing to construct a water Cherenkov extensive air shower array at the Sierra Negra site in Mexico. The altitude of the observatory would be 4100 m above sea level. In addition to the increased altitude the response of HAWC will be further improved (relative to Milagro) by the optical isolation of each detection cell, and a factor of ~ 10 increase in the size of the muon detection area. A schematic of the HAWC is shown in Fig. 11. HAWC will be composed of 900 large water tanks. Each tank will be 4.3 meters tall and have a diameter of 5 m. The tanks will be instrumented with a single 8 inch Hamamatsu R5912 PMT placed at the bottom, looking up at the water volume. The tanks will be arranged in a close packed grid with space between every other row for moving equipment. The total area of the array will be $150\text{m} \times 150\text{m}$, with a 78% active detection area. The total project cost is roughly \$9M USD.

Unlike Milagro, HAWC has a single PMT in each cell. Signals from this single layer are used to both reconstruct the direction of the primary cosmic ray and gamma ray, and to distinguish the gamma-ray events from the hadronic cosmic-ray induced events. This combined with a larger cell separation (2.8 m in Milagro) allows for a much larger (densely instrumented) detector area. The total instrumented area of HAWC ($22,000\text{ m}^2$) is

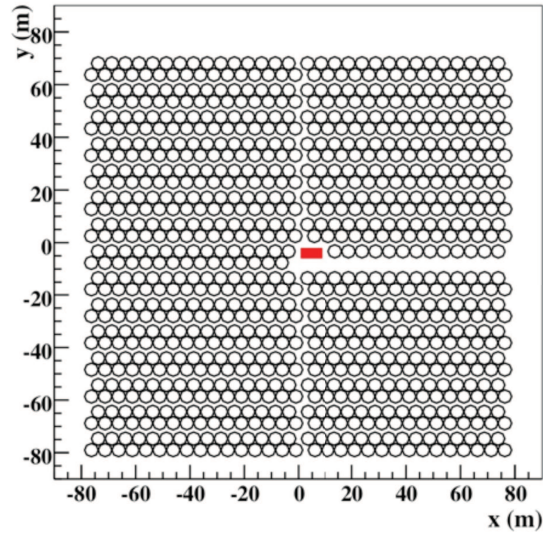


Fig. 11. The HAWC detector. Each tank measures 4.3 m tall by 5 m diameter. The tanks are arranged in a close-packed grid with 5m spacing between tanks.

comparable to that of Milagro including the trigger array. But in Milagro only the central $4,000\text{ m}^2$ reservoir is used for triggering, and the muon detection area is the size of the bottom of the reservoir, 2300 m^2 . The combination of higher altitude and larger trigger area lead to a substantial increase in the effective area for lower energy gamma rays of HAWC relative to Milagro. Fig. 12 shows the effective area as a function of primary gamma-ray energy for HAWC and Milagro. For both detectors two curves are given. The higher (solid) curve shows the effective area before a cut is applied to distinguish gamma rays from the hadronic background. The dashed curve shows the effective area after the background rejection cut is applied.

From the figure it can be seen that the gamma-ray efficiency of the background rejection cut is much higher in HAWC, especially at low energies. This is due to the fact that at low energies most of the gamma-ray events that trigger Milagro have the shower core within the central reservoir. The core of a gamma-ray shower gives significant light yield in the bottom layer of the reservoir and therefore these events fail the background rejection cut. In HAWC, because of the larger size of the array, cells within 30 meters of the reconstructed shower core are excluded from the back-

ground rejection algorithm. (In Milagro this area is comparable to the total area of the bottom layer.) Therefore, the background rejection cut does not reject low-energy gamma rays in HAWC, leading to a substantial improvement in the effective area of HAWC at low energies and a commensurate improvement in the sensitivity to distant objects such as gamma-ray bursts. Figure 13 shows the efficiency for retaining hadronic events as a function primary energy for HAWC and Milagro. The rejection parameter used is similar in the two cases with the addition of the exclusion of PMTs within 30m of the fit shower core in the case of HAWC. The large gain in background rejection capability is mostly due to the 10-fold increase in the size of the deep layer in HAWC relative to Milagro. It should be noted that at the highest energies insufficient Monte Carlo data has been generated to properly estimate the true capabilities of HAWC to reject the cosmic-ray background. The numbers presented in Fig. 13 are upper limits to the hadron efficiency as no hadronic events survived the background rejection cuts at energies above ~ 50 TeV. While it is beyond the scope of this paper to discuss this at length, it is likely that HAWC will be in a background free regime above ~ 100 TeV. This is also true for the Tibet array with added muon detectors (discussed below).

In addition, the larger array size leads to a larger lever arm that can be used in reconstructing the direction of events. This leads to an improvement in the angular resolution of HAWC relative to Milagro by about 40% overall. (The improved angular resolution is a function of primary gamma-ray energy and is most pronounced at low energies.) The combination of the above three factors, increased area (due to higher altitude and larger area of dense coverage), increased size of muon detection layer, and increased angular resolution, lead to a 15-fold increase in sensitivity relative to Milagro.

An alternative approach to the future of all-sky, ground-based gamma-ray observatories is to dramatically improve upon the sensitivity at the highest energies. The combination of large aperture and continuous observation gives such instruments distinct advantages over air Cherenkov telescopes in studying the highest energy gamma rays. For example, once one attains a background free regime,

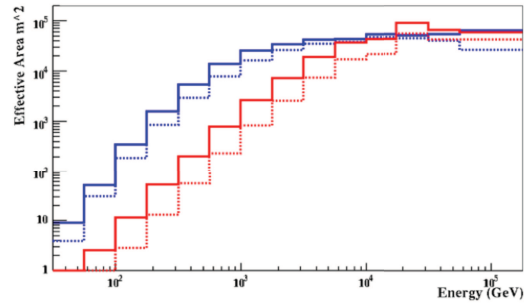


Fig. 12. The effective area of the HAWC (blue/upper lines) and Milagro (red/lower lines) detectors. The solid lines show the area before background rejection cuts have been applied and the dashed lines after these cuts are applied. In both cases only events that are successfully reconstructed, within the analysis bin are counted.

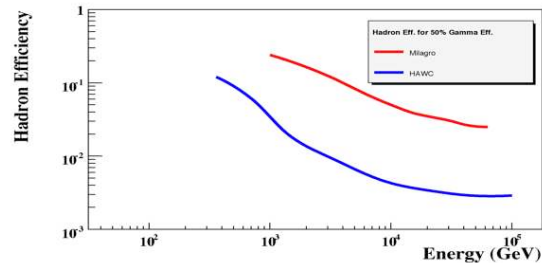


Fig. 13. The efficiency for retaining events generated by hadronic cosmic rays for HAWC and Milagro. In both cases the hadron efficiency is given for a cut level that retains 50% of the gamma ray events.

the sensitivity of a detector is determined simply by the number of gamma rays one can detect from a given source. This in turn is simply the product of the effective area of the detector at the highest energies and the amount of time one can spend on source. While an IACT with a dedicated observation program may attain 50-100 hours on source for a small number of objects, ~ 5 , in year, an EAS type array will obtain about 1600 hours on source for *all* objects within its field-of-view (typically all objects with a declination within 45 degrees of the latitude of the detector). Therefore at the highest energies an all-sky detector will always have the advantage over an IACT, if it has the ability to reject all of the hadronic background events. This is the approach taken by the Tibet AS γ collaboration and the instrument will be referred to as Tibet MD. The Tibet MD collaboration is planning on

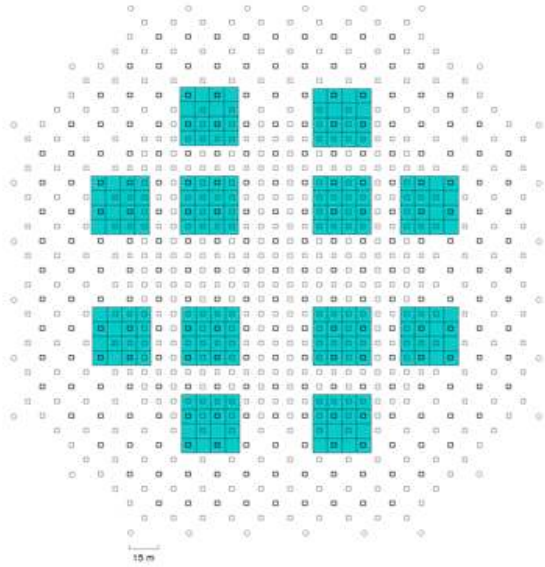


Fig. 14. Schematic view of the Tibet MD array with the proposed muon detectors. The muon detectors are buried under 2.5m of dirt.

installing over 9500 m^2 of muon detector within the existing $\text{AS}\gamma$ array [36, 37]. Fig. 14 shows the proposed layout of the detector. The muon detectors are water Cherenkov counters buried under 2.5 m of dirt. Each counter consists of a water pool measuring $7.2\text{m} \times 7.2\text{m} \times 1.5\text{m}$ deep, instrumented with two 20-inch Hamamatsu R3600 PMTs. The water pools are made from concrete and painted with a white epoxy resin. With this area of muon detector, the Tibet $\text{AS}\gamma$ collaboration expects to be background free near $\sim 200 \text{ TeV}$. Since the existing Tibet array is about twice the size of the proposed HAWC detector, this array will have the highest sensitivity of any existing or proposed instrument above about 20 TeV .

These two future projects will give us an unprecedented view of the high-energy universe. With its low-energy response and high sensitivity extending to beyond 100 TeV , HAWC will be able to observe many flaring active galaxies, possibly detect the highest energy emission from gamma-ray bursts, and make a detailed map the Galaxy in TeV gamma rays. The Galactic diffuse flux will be measured and mapped between 1 and 100 TeV , with exquisite spatial precision. By coupling the TeV diffuse maps with those made by the GLAST

instrument our understanding the cosmic-ray population throughout the Galaxy will make significant advances. At the highest energies Tibet MD will study the end-point spectra of many Galactic objects. Their sensitivity is sufficient to detect most of the hard spectrum HESS sources above 100 TeV (if their power-law spectra continue to these energies).

Conclusions

All-sky TeV gamma-ray observatories have made significant observations over the past five years. The previous generation of instruments lacked the sensitivity required detect even a single source of TeV gamma rays. The technological advance that made much of these detections possible was the application of water Cherenkov technology to the field. By enabling the dense sampling required to detect essentially all of the electromagnetic particles in the air shower (both gamma rays and electrons), and simultaneously providing a large area muon detector, this technology dramatically reduced the energy threshold of all-sky instruments. An alternate approach that has resulted in only slightly degraded sensitivity relative to the water Cherenkov approach was to go to an extreme altitude and construct a relatively dense scintillator array. Both approaches have resulted in significant observations.

The first detection of the Galactic diffuse emission above a TeV has indicated that the cosmic-ray spectrum may vary throughout the Galaxy and has given an indication of the location of possible cosmic-ray acceleration sites (the Cygnus Region). A class of extended sources has also been discovered, most of which are coincident with GeV sources detected by EGRET. It is likely that these are pulsar wind nebula, indicating that these sources have very hard spectra and the ability to accelerate particles to at least 20 TeV . Perhaps the most exciting discovery is of MGRO J1908+06. This discovery by the Milagro collaboration was followed up by H.E.S.S. observations. The H.E.S.S. observations made several important demonstrations: 1. The agreement between the spectrum measured by H.E.S.S. and the flux measured by Milagro showed that the two techniques are in fact relatively calibrated to within at least

20%, 2. The determination by H.E.S.S. that the source is in fact extended, validated the Milagro measurement and demonstrated the reality of the other extended sources discovered by Milagro, and 3. The H.E.S.S. spectrum is very hard, E^{-2} , and the Milagro data suggest that at least up to 50 TeV there is no change in the spectral index. Milagro should follow-up on this analysis and could have the ability to measure the spectrum of this source to 100 TeV. This could be the highest energy accelerator detected to date and again an excellent candidate for a cosmic-ray acceleration site. Finally, both Tibet and Milagro have detected emission from extragalactic objects, demonstrating the capability of future all-sky instruments.

Fig. 15 shows the point-source sensitivity of current and future all-sky gamma-ray instruments. For comparison the sensitivity of GLAST and VERITAS/H.E.S.S. are shown. For the all-sky instruments the sensitivity is calculated for a year exposure and averaged over the field-of-view of the instruments. The all-sky instruments can observe at least 2π sr of the sky with this level of sensitivity. (GLAST will survey the entire 4π sr of the sky with the level of sensitivity indicated.) In contrast the sensitivity of the IACTs is given for a 50 hour exposure. With a 10% duty cycle and a field-of-view of 2-3 msr, they can observe less than 45 msr of the sky with this level of sensitivity in a single year. Therefore it is clear that the field of gamma-ray astronomy requires both types of instruments to gain a true understanding of the high-energy universe. The IACTs have unrivaled angular resolution (0.05-0.1 degrees) and therefore the capability to map extended Galactic sources. This capability coupled with x-ray, optical, and radio maps will certainly lead to a much better understanding of the individual sources. The IACTs also have significantly better energy resolution than the all-sky instruments. In addition to enabling a better understanding of astrophysical sources, this also enables them to excel at the identification of dark matter annihilation, if such a phenomena is observed. However, the all-sky instruments have the unique capability to simultaneously view a huge region of the sky. This feature alone makes them uniquely suited to detecting transient phenomena in the high-energy universe. Despite over a decade of study since the first detection of an extragalactic

object [38] we still do not know the duty cycle of TeV flaring activity in active galaxies and we have yet to detect >100 GeV emission from gamma-ray bursts. The next generation of all-sky instruments hold the promise of enabling such observations. Given the observed flaring nature of the known active galaxies it is expected that an instrument such as HAWC will detect many TeV flares in a single year. Furthermore, the high-energy domain above a few TeV is the region where the all-sky instruments will dominate. These new instruments will provide an unprecedented view of the Galactic diffuse emission that will lead to a better understanding of the distribution and spectrum of cosmic rays throughout our Galaxy (both cosmic-ray hadrons and electrons). If this next generation of all-sky instruments is constructed the next decade will be an exciting time for the gamma-ray community and we can look forward to a decade of discovery at the high-energy frontier.

Acknowledgements

This work is partially supported by the National Science Foundation, the Department of Energy Office of Science, and Los Alamos National Laboratory. I would like to thank Zhen Cao and for his assistance with information regarding the ARGO detector and Hu Hongbo for his help in understanding the Tibet AS γ detector. I would also like to thank and acknowledge all of my colleagues working on the Milagro Observatory without whom these beautiful results would not have been possible.

References

- [1] D.E. Alexandreas, et al., Nucl. Instrum. Meth. A 328 (1993) 570.
- [2] A. Borione, et al., Nucl. Instrum. Meth. A 346 (1994) 329.
- [3] R.W. Atkins, et al., Astrophys. J. 595 (2003) 803.
- [4] M. Amenomori, et al., Proceedings of the 29th ICRC, Pune, India, 2005.
- [5] M. Amenomori, et al., Astrophys. J. 525 (1999) L93.
- [6] M. Amenomori, et al., Proceedings of the 29th ICRC, 2005, Pune, India, 2005.

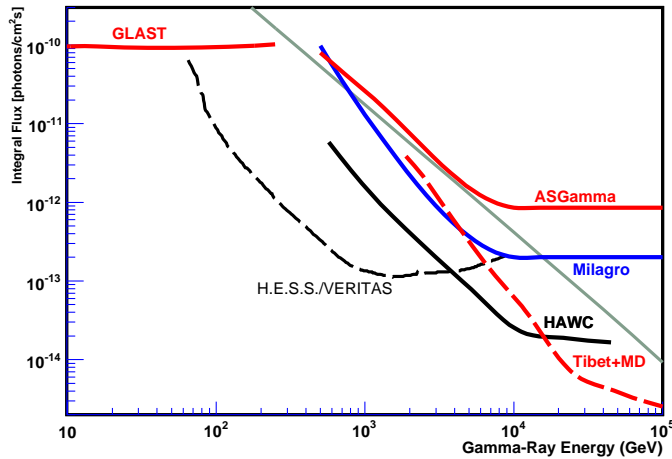


Fig. 15. Point source sensitivity of current and future gamma-ray observatories. For pointed instruments (H.E.S.S./VERITAS) the sensitivity is shown for a 50 hour exposure to a single source (using all available observing time in a year 15 points in the sky can be observed with this level of sensitivity). For all-sky instruments such as GLAST, Tibet, and HAWC the sensitivity is shown averaged over the entire visible sky (typically 2π sr) for a one-year exposure.

- [7] A.A. Abdo, et al., *Astrophys. J.* 658 (2007) L33.
- [8] A. Aloisio (ARGO collaboration), *Proceedings of the 30th ICRC, Merida, Mexico, 2007, Vol. 5, p. 1065.*
- [9] R. W. Atkins, et al., *Astrophys. J.* 608 (2004) 680.
- [10] G. Sinnis (Milagro collaboration), *Proceedings of the American Physical Society, 2002.*
- [11] A. Falcone, et al., *Proceedings of the 28th ICRC, Tsukuba, Japan, 2003.*
- [12] G. Walker, R. Atkins and D. Kieda, *ApJL.* 614 (2004) L93.
- [13] M. Amenomori, et al., *Proceedings of the 29th ICRC, Pune, India, 2005.*
- [14] R.C. Hartman, et al., *ApJS.* 123 (1999) 79.
- [15] F. Aharonian, et al., *Astron. Astrophys.* 431 (2005) 197.
- [16] R.C. Lamb and D.J. Macomb, *ApJ.* 488 (1997) 872.
- [17] A.A. Abdo, et al., *ApJL.* 664 (2007) L92.
- [18] K.A. van der Hucht, *New Astron. Rev.* 45 (2001) 135.
- [19] N.G. Bochkarev and T.G. Sitnik, *Astrophys. Space. Sci.* 108 (1985) 925.
- [20] D.A. Green, *Bull. Astron. Soc. India,* 32 (2004) 325.
- [21] A.A. Abdo, et al., *ApJL.* 658 (2007) L33.
- [22] R. Mukherjee, et al., *ApJ.* 542 (2000) 740.
- [23] F. Aharonian, et al., *Astron. & Astrophys.* 431 (2005) 197.
- [24] Ona-Wilhemi (HESS collaboration), *Proceedings of the 30th ICRC, Merida, Mexico, 2007, Vol. 2, p. 863.*
- [25] S.D. Hunter, et al., *ApJ.* 481 (1997) 205.
- [26] W. de Boer, et al., *Astron. & Astrophys.* 444 (2005) 51.
- [27] A.W. Strong, I.V. Moskalenko and O. Reimer, *ApJ.* 613 (2004a) 962.
- [28] A.W. Strong, et al., *Astron. & Astrophys.* 422 (2004b) L47.
- [29] P. Gralewicz, et al., *Astron. & Astrophys.* 318 (1997) 925.
- [30] P. Huentemeyer (Milagro collaboration), *Proceedings of the 30th ICRC, Merida, Mexico, 2007, Vol. 2, p. 509.*
- [31] D.L. Hall, M.L. Duldig, and J.E. Humble, *Space Science Reviews* 78 (1996) 401.
- [32] M. Amenomori, et al., *Science* 314 (2006) 439.
- [33] A.H. Compton and I.E. Getting, *Phys. Rev.* 47 (1935) 817.
- [34] G. Walker (Milagro collaboration), *Proceedings of the 30th ICRC, Merida, Mexico, 2007, Vol. 2, p. 513.*
- [35] M.M. Gonzalez (HAWC collaboration), *Pro-*

- ceedings of the 30th ICRC, Merida, Mexico, 2007, Vol. 3, p. 1567.
- [36] S. Takashi (Tibet AS γ collaboration), Proceedings of the 30th ICRC, Merida, Mexico, 2007, Vol. 2, p. 353.
- [37] S. Takashi (Tibet AS γ collaboration), Proceedings of the 30th ICRC, Merida, Mexico, 2007, Vol. 2, p. 357.
- [38] M. Punch, et al., Nature 358 (1992) 477.